A Combustion Stability Analysis for Catalytic Monopropellant Thrusters

W. L. OWENS, Jr.*
Lockheed Missiles & Space Company, Sunnyvale, Calif.

An analytical means of determining the low-frequency combustion stability for catalytic monopropellant thrusters has been presented. The use of frequency-analysis from feedback control systems is shown to predict the conditions of stable-unstable operation of a 200lbf hydrazine thruster. The open-loop transfer function for system response was obtained from the feedline and thruster equations for a pressure-fed, flexibly mounted thruster. The resulting set of six equations in six unknowns was normalized using the steady-state mass rate and chamber pressure. The open-loop character of the linearized, transformed equations was obtained from a stability analysis digital computer program. Experimental stable-unstable operation of a 200lbf hydrazine thruster was correlated by a 12 msec value of combustion time delay determined from the analysis. The analytical value of combustion time delay was shown to be in good agreement with experimental values determined by the method of flow-interruption. A simpler solution for a rigidly mounted thruster is also presented which allows rapid graphical determination of combustion stability.

Nomenclature

A = area
A^* = nozzle throat area
C^* = characteristic velocity
C_F, C_W = thrust, mass flow coefficient
D_M = mount damping coefficient
g_c = conversion factor in Newton's law of motion
H = frictional head loss
I_S = specific impulse
K_M = mount spring constant
L = length
L^* = characteristic chamber length
M_T = thruster mass
$\dot{m}$ = mass rate
P = pressure
R = gas constant
S = Laplace transformation variable
T = temperature
t = time
V = volume
V_B = bed void volume
X = thruster and bellows displacement
κ = propellant compressibility
μ = mass rate ratio
ρ = propellant density
τ = combustion time delay
φ = pressure ratio
Ω = function of specific heat ratio
$\bar{}$ = bar over term signifies steady-state value

Subscripts

1,2 = sections of feedline
B = catalyst bed
C = chamber
F = flexible bellows
L = feedline
T = tank and thruster

Presented as Paper 71-701 at the AIAA/SAE 7th Propulsion Joint Specialist Conference, Salt Lake City, Utah, June 14-18, 1971; submitted June 21, 1971; revision received October 26, 1971.

* Staff Engineer, Propulsion Systems, Space Systems Division. Member AIAA.

Introduction

THE increasing use of monopropellant hydrazine with the Shell 405 catalyst in gas generators and thrusters has generated the need for predicting the conditions for stable operation of these systems. Low-frequency instability for thermal decomposition monopropellant thrusters is well known, having been studied and described by Summerfield and Crocco.[1,2] They demonstrated, along with others, the significance of the hydraulic coupling between the feedline and chamber when a combustion time delay is present. It was shown that these factors could lead to a chugging type of instability when the proper conditions were met. The problem of low-frequency instability for catalytic monopropellant thrusters is fundamentally the same as that for thermal decomposition chambers. The primary difference is the additional pressure loss and capacitance effect resulting from the inclusion of a catalyst bed in the chamber.

The present approach to calculating the conditions for low-frequency instability is similar to that used previously to analyze pogo oscillations in liquid rocket vehicles.[3,4] The linearized equations for the various system elements are written in normalized form and the open-loop character of the transformed equations is then analyzed for gain and phase angle using the method of frequency-analysis from feedback control systems.[5]

Analysis

The thruster is assumed to be flexibly mounted and connected to a rigidly mounted tank through a bellows in the feedline as shown in Fig. 1. Oscillation of the thruster produces a pumping action in the bellows which can influence feedline dynamics. It is assumed that the tank feed pressure is quasi-static along with incompressible flow in the feedline and the absence of body forces.

The gas within the catalyst bed is assumed to be at an average density given by the arithmetic average of the bed inlet and exit pressure, and an average temperature and molecular weight given by the characteristic velocity. The actual conditions within the bed are known to vary with position as demonstrated by MacLean and Wagner for hydrazine decomposition flames.[6] An analytical solution for catalyzed hydrazine reaction chambers shows the gas composition and temperature can be a function of radial as

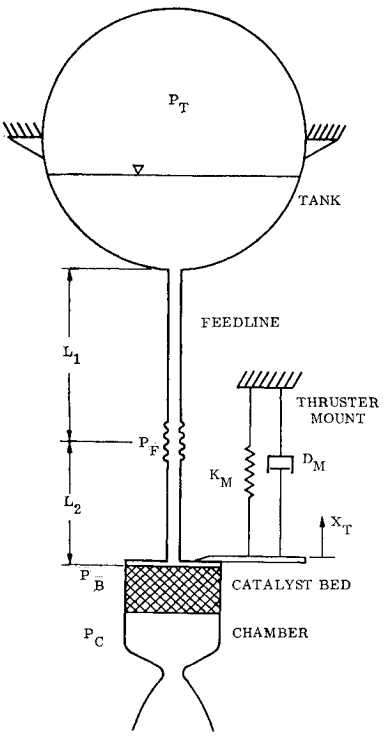

Fig. 1 Schematic of catalytic monopropellant propulsion system.

well as axial position, depending on the manner of injection.[7] The effective combustion time delay would also be expected to vary with the method of injection, bed reactivity, pressure and temperature, and composition profile. The present analysis indicates that use of an average bed gas density can generally be justified on the basis of its second-order effect on the conditions for stability.

Feedline Equations

The expression for the liquid inertial effects in the feedline is obtained from the momentum theorem where the summation of forces is given by the pressure and viscous drag forces. Neglecting the time rate of change of momentum in the tank, the expression for section L_1 of Fig. 1 is given by

$$\frac{L_1}{g_c A_1}\frac{d\dot{m}_1}{dt} = P_T - P_F + \frac{\dot{m}_1^2}{2g_c\rho}\left(\frac{1}{A_T^2} - \frac{1}{A_F^2}\right) - \rho H_1 \qquad (1)$$

Equation (1) can be normalized to the form

$$(C_w A^* L_1/g_c A_1)(d\mu_1/dt) = \varphi_T - \varphi_F - (\overline{\Delta P_1}/\bar{P}_c)\mu_1^2 \qquad (2)$$

where

$$\mu_1 = \dot{m}_1/\bar{m}, \qquad \varphi_F = P_F/\bar{P}_c, \qquad H_1 \propto \dot{m}_1^2$$

The same type of equation can be written for section L_2.

$$(C_w A^* L_2/g_c A_2)(d\mu_2/dt) = \varphi_F - \varphi_B - (\overline{\Delta P_2}/\bar{P}_c)\mu_2^2 \qquad (3)$$

The expression for the time derivative of the bellows pressure is obtained from the continuity equation.

$$dP_F/dt = (1/\rho V_F \kappa)(\dot{m}_1 - \dot{m}_2 + \rho A_F \dot{X}_T) \qquad (4)$$

Normalizing Eq. (4) yields

$$(\rho V_F \kappa/C_w A^*)(d\varphi_F/dt) = \mu_1 - \mu_2 + \mu_F \qquad (5)$$

where

$$\mu_F = \rho A_F \dot{X}_T/C_w A^* \bar{P}_c$$

Thruster Mount Equation

A force balance on the thruster, neglecting the bellows momentum flux and liquid inertial effects, yields the differential equation for thruster displacement

$$(M_T/g_c)\ddot{X}_T = C_F A^* P_C - K_M X_T - D_M \dot{X}_T - P_F A_F \qquad (6)$$

Equation (6) can be written in terms of μ_F to yield the following expression:

$$\frac{M_T}{g_c \rho A_F I_S}\frac{d\mu_F}{dt} = \varphi_C - \frac{K_M}{\rho A_F I_S}\int \mu_F\, dt - \frac{D_M}{\rho A_F I_S}\mu_F - \frac{A_F}{C_F A^*}\varphi_F \qquad (7)$$

Combustion Chamber Equations

The time derivative of the catalyst bed pressure is obtained from the continuity equation, where the injected propellant is assumed to require a period of time τ before it instantaneously decomposes, and thus

$$V_B(d\rho_B/dt) \equiv (V_B/2RT)[(dP_B/dt) + (dP_C/dt)] = \dot{m}_2(t-\tau) - \dot{m}_B \qquad (8)$$

It is assumed that the relationship between bed mass rate and pressure drop is given by

$$\dot{m}_B^2 \propto (P_B - P_C)$$

Substituting for bed mass rate in Eq. (8) and normalizing yields

$$\frac{L_B^*}{2\Omega^2 C^*}\left(\frac{d\varphi_B}{dt} + \frac{d\varphi_C}{dt}\right) = \mu_2(t-\tau) - \left[\frac{\bar{P}_C}{\overline{\Delta P_B}}(\varphi_B - \varphi_C)\right]^{1/2} \qquad (9)$$

The expression for the chamber is similarly obtained and is given by

$$(L_C^*/\Omega^2 C^*)(d\varphi_C/dt) = [(\bar{P}_C/\overline{\Delta P_B})(\varphi_B - \varphi_C)]^{1/2} - \varphi_C \qquad (10)$$

System of Equations

The preceding derivation results in six equations in six unknowns. Linearization of the feedline and chamber equations is accomplished by using the approximation $\mu^2 \approx 2\mu - 1$. The error associated with this substitution is given by $(\mu - 1)^2$, which is small for values of μ close to unity.

The system of linearized equations is as follows:

$$F_1(d\mu_1/dt) = \varphi_T - \varphi_F - 2E_1\mu_1 + E_1 \qquad (11)$$

$$F_2(d\mu_2/dt) = \varphi_F - \varphi_B - 2E_2\mu_2 + E_2 \qquad (12)$$

$$M(d\mu_F/dt) = \varphi_C - G\int \mu_F dt - H\mu_F - J\varphi_F \qquad (13)$$

$$N(d\varphi_F/dt) = \mu_1 - \mu_2 + \mu_F \qquad (14)$$

$$(B/2)[(d\varphi_B/dt) + (d\varphi_C/dt)] = \mu_2(t-\tau) - 0.5D(\varphi_B - \varphi_C) - 0.5 \qquad (15)$$

$$C(d\varphi_C/dt) = 0.5D(\varphi_B - \varphi_C) - \varphi_C + 0.5 \qquad (16)$$

$$B = L_B^*/\Omega^2 C^*,\ C = L_C^*/\Omega^2 C^*,\ D = \bar{P}_C/\overline{\Delta P_B},\ E = \overline{\Delta P_L}/\bar{P}_C,$$

$$F = C_w A^* L/g_c A_L,\ G = K_M/\rho A_F I_S,\ H = D_M/\rho A_F I_S,$$

$$J = A_F/C_F A^*,\ M = M_T/g_c \rho A_F I_S \text{ and } N = \rho V_F \kappa/C_w A^*$$

The various system interactions of the six linear differential equations given above are shown in analogue form in Fig. 2.

Open-Loop Response

The open-loop response of this system is obtained through the Laplace transformation of Eqs. (11–16) and determination of the denominator of the resulting subsidiary equation for

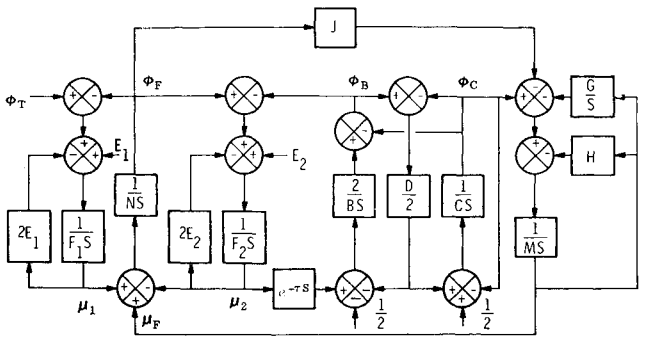

Fig. 2 Linearized thruster system analogue.

any of the six variables. The expression for the open-loop transfer function can be shown to result from the following matrix equation when solved for $\mu_2(S)$:

$$\begin{bmatrix} F_1S+2E_1 & 0 & 0 & 1 \\ 0 & F_2S+2E_2 & 0 & -1 \\ 0 & 0 & MS^2+HS+G & JS \\ -1 & 1 & -1 & NS \\ 0 & 0 & 0 & 0 \\ 0 & 0 & 0 & 0 \end{bmatrix} \begin{bmatrix} 0 & 0 \\ 1 & 0 \\ 0 & -S \\ 0 & 0 \\ (BS+D)/2 & (BS-D)/2 \\ -D/2 & CS+1+D/2 \end{bmatrix} \begin{bmatrix} \bar{\mu}_1(S) \\ \bar{\mu}_2(S) \\ \bar{\mu}_F(S) \\ \bar{\varphi}_F(S) \\ \bar{\varphi}_B(S) \\ \bar{\varphi}_C(S) \end{bmatrix} = \begin{bmatrix} 0 \\ 0 \\ 0 \\ 0 \\ -e^{-\tau S} \\ 0 \end{bmatrix}$$

In determinate form, the open-loop transfer function is given by $-A_{52}e^{-\tau S}/|D|$, where A_{52} is the cofactor of the fifth row and second column and $|D|$ is the value of the determinate. Calculation of gain and phase angle were accomplished using the LMSC General Stability Analysis Digital Computer Program.

Stability for Rigidly Mounted Thruster

Considering the thruster to be rigidly mounted simplifies the solution for stability to the extent of eliminating three of the six equations previously derived. The system of equations for this condition is given by

$$F(d\mu_L/dt) = \varphi_T - \varphi_B - 2E\mu_L + E \tag{17}$$

together with Eqs. (15) and (16).

The open-loop expression is relatively simple in this case and is given by

$$\frac{1+0.5D}{DE}\,\frac{(T_1S+1)e^{-\tau S}}{(T_2S+1)(T_3S+1)(T_4S+1)} \tag{18}$$

where

$$\frac{1}{T_1}=\frac{1+0.5D}{C}, \qquad \frac{1}{T_2}=\frac{2E}{F}$$

$$\frac{1}{T_3}=\frac{B(1+D)+CD}{2BC}\left[1+\left(1-\frac{4BCD}{[B(1+D)+CD]^2}\right)^{1/2}\right]$$

$$\frac{1}{T_4}=\frac{B(1+D)+CD}{2BC}\left[1-\left(1-\frac{4BCD}{[B(1+D)+CD]^2}\right)^{1/2}\right]$$

The condition of marginal stability results from the characteristic equation having complex conjugate roots on the imaginary axis with all other roots in the left half of the S plane. This may be determined from the Nyquist criterion using the frequency-analysis method for linear systems. The stability of a particular system can be readily determined from a Bode plot of its frequency response, using the four corner frequencies and gain computed for particular values of B, C, D, E, and F. The zero dB gain condition may be obtained by setting the frequency invariant factors of Eq. (18) equal to one.

$$1+0.5D=DE \quad \text{or} \quad \bar{P}_c=2(\overline{\Delta P_L}-\overline{\Delta P_B})$$

A sufficient condition for stability is then given by

$$\overline{\Delta P_L}-\overline{\Delta P_B}>0.5\bar{P}_c \tag{19}$$

For the case of zero bed pressure drop, this expression reduces to Eq. (19) of Ref. 1 for monopropellant thermal decomposition chambers.

Analytical Correlation of Experimental Data

Experimental stability data for a 200lbf hydrazine thruster were used to verify the general utility of the preceding analysis over a fairly wide range of operating conditions. These data were obtained from Ref. 8 for a flexibly mounted, pressure-fed hydrazine thruster similar in arrangement to the schematic of Fig. 1. The feedline contained a flowmeter and valve in addition to a flexible bellows. The propellant injector was of the penetration type with 19 slotted tubes extending from the manifold to the catalyst bed retainer. Each of the injector tubes was surrounded by a cylindrical wire screen partition containing 20–24 mesh Shell 405 catalyst. The remainder of the bed contained 8–12 mesh Shell 405 catalyst, yielding a maximum bed loading of approximately 3lbm/min-in.[2]

Lacking a value of combustion time delay for thrusters of this type, the analysis was used to determine a value which would provide a correlation of the stable-unstable operating regimes. The analytical value was subsequently verified by combustion time delay data obtained from a thruster of the same design.

The General Stability Analysis Digital Computer Program was used to determine values of τ which produced marginal stability for a range of values of the two independent variables, $\bar{P}_c/\overline{\Delta P_L}$ and $\bar{P}_c/\overline{\Delta P_B}$. The results are shown in Fig. 3 along with values of the constants used in Eqs. (11–16) calculated for the thruster of Ref. 8. For any particular value of combustion time delay in Fig. 3, values of $\bar{P}_c/\overline{\Delta P_L}$ and $\bar{P}_c/\overline{\Delta P_B}$ to the right theoretically yield stable operation while values to the left produce instability. The stable-unstable

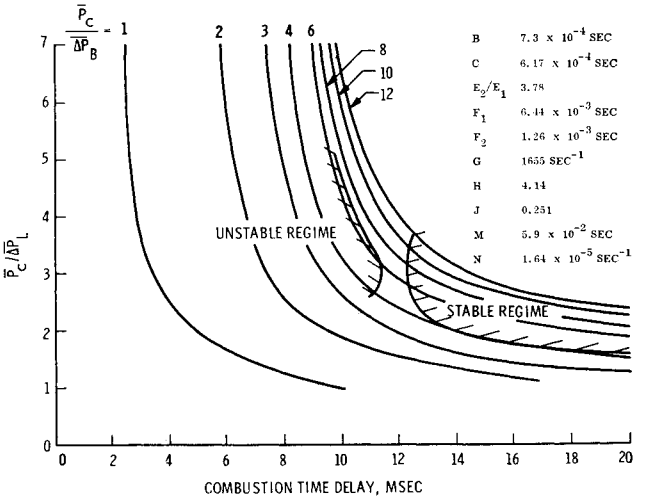

Fig. 3 Analytical determination of combustion time delay for a 200lbf hydrazine thruster.

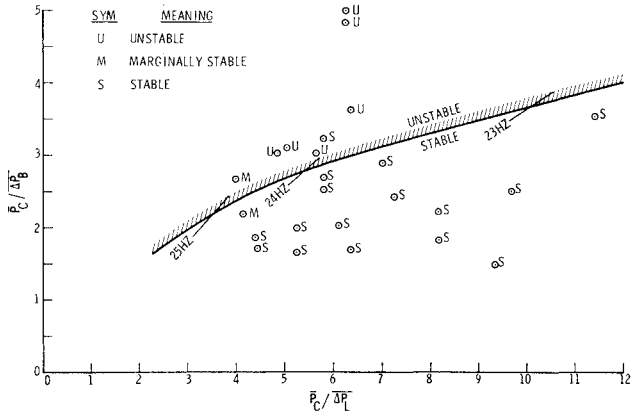

Fig. 4 Comparison of predicted stable-unstable boundary for a τ of 12 msec with experimental data for a 200lbf hydrazine thruster.

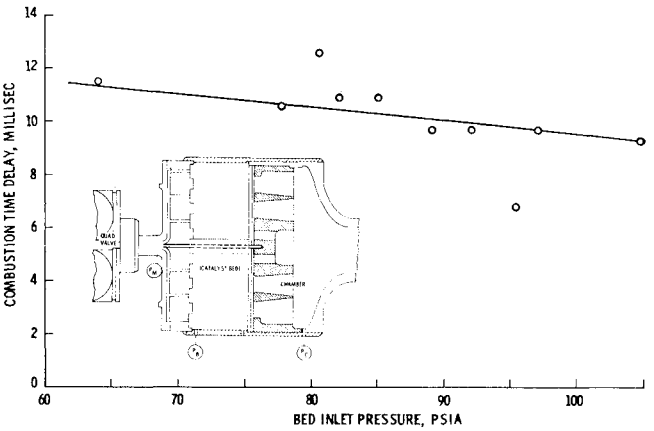

Fig. 6 Combustion time delay vs bed pressure for a 250lbf hydrazine thruster of the design shown.

operating regimes for the 200lbf thruster were established in Fig. 3 using the experimental data points shown in Fig. 4. From these, a value of approximately 12 msec was obtained to satisfy the condition of marginal stability. Figure 4 shows the individual data points along with the analytically determined boundary and frequencies for marginal stability using a combustion time delay of 12 msec.

Discussion

With one exception, the analysis bounds stable and unstable operation for the 200lbf thruster data shown in Fig. 4. This correlation was forced to the extent that the value of combustion time delay was arbitrarily chosen from Fig. 3 to predict the condition of marginal stability. In order to give increased confidence in the analytical method, it was felt necessary to show agreement between the analytical and actual combustion time delay. Several methods are available for obtaining experimental values of τ. One approach is the rather complicated method of modulated injection after Crocco, et al.[9] A somewhat simpler method is that of flow interruption described in Barrére.[10] This consists of determining the time lapse between flow termination and the beginning of chamber pressure decay from which an estimate of τ may be obtained. Figure 5 shows a typical oscillograph trace for flow termination of a 250lbf hydrazine thruster of the same design as Ref. 8. The location of the various pressure taps and bed configuration are shown in Fig. 6

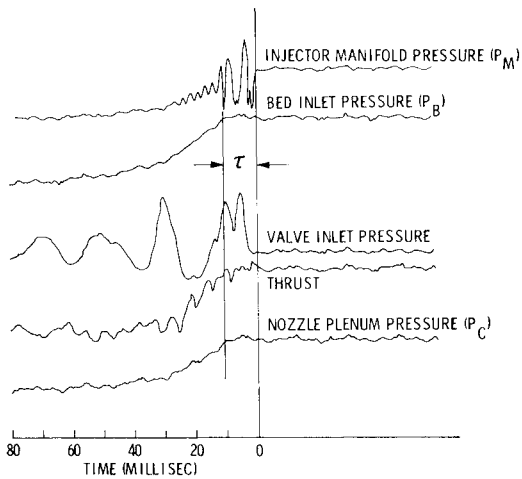

Fig. 5 Typical oscillograph pressure-time traces for flow interruption of a 250lbf hydrazine thruster.

along with measured values of τ as a function of bed inlet pressure. The instant of flow termination was assumed to be given by the drop in injector manifold pressure shown in Fig. 5 at time zero. The interval τ represents the time required for the propellant within the bed to decompose before bed and chamber pressure begin to decay. The values of τ obtained from both the bed and chamber pressure traces were in close agreement; also, the values shown in Fig. 6 are felt to be accurate within approximately one msec. The low value of τ at a bed pressure of 95 psia was characteristic of the initial firing for a new thruster. All of the data shown were for firing durations in excess of 40 sec prior to shutdown.

The agreement between the analytically determined value of 12 msec and the experimental data of Fig. 6 is felt to be very good. The unstable operation shown in Fig. 4 occurred over an approximate bed inlet pressure range of 50–70 psia which would indicate a value of τ between 11 and 12 msec from Fig. 6. In addition, the experimental frequencies for the data of Fig. 4 were generally in the range of 15–20 Hz which was on the order of that calculated for marginal stability.

The analysis indicates that combustion stability may be improved by an increase in feedline and injector pressure drops and/or a decrease in catalyst bed drop. Stability is also sensitive to combustion time delay and decreasing τ through injector design or bed reactivity will result in improved stability. The influence of a bellows and flexible thruster mount can be stabilizing or destabilizing for a particular design, depending on the combustion time delay, oscillation frequency and phase angle, and bellows and feedline dynamics. The general influence of feedline, catalyst bed, and chamber can be ascertained from the four corner frequencies listed after Eq. (18) for a rigidly mounted thruster.

Conclusions

It is felt that the good agreement between the analysis and experimental stability data for a fairly complicated monopropellant hydrazine thruster generally substantiates the use of the present approach. Successful extension of this method to other thrusters would provide increased confidence in its ability to predict stable-unstable operation over a greater range of conditions. The majority of cases should allow the use of Eq. (18) to establish the conditions for stable operation whenever the inequality of Eq. (19) cannot be satisfied for a rigidly mounted thruster. Use of Bode plots with the four corner frequencies, should allow rapid calculation of stability for a particular system and range of operating conditions.

References

[1] Summerfield, M., "A Theory of Unstable Combustion in Liquid Propellant Rocket Systems," *ARS Journal*, Vol. 21, No. 5, Sept. 1951, pp. 108–114.

[2] Crocco, L., "Aspects of Combustion Stability in Liquid Propellant Rocket Motors," Part 1, *ARS Journal*, Vol. 21, No. 6, Nov. 1951, pp. 163–178.

[3] McKenna, K. J., Walker, J. H., and Winje, R. A., "Engine-Airframe Coupling in Liquid Rocket Systems," *Journal of Spacecraft and Rockets*, Vol. 2, No. 2, March-April 1965, pp. 254–256.

[4] Rubin, S., "Longitudinal Instability of Liquid Rockets Due to Propulsion Feedback (*POGO*)." *Journal of Spacecraft and Rockets*, Vol. 3, No. 8, Aug. 1966, pp. 1188–1195.

[5] Savant, C. J., Jr., "*Basic Feedback Control System Design*," McGraw-Hill, New York, 1958, pp. 124–168.

[6] MacLean, D. I. and Wagner, H. Gg, "The Structure of the Reaction Zones of Ammonia-Oxygen and Hydrazine-Decomposition Flames," *Eleventh Symposium (International) on Combustion*, The Combustion Institute, 1967, p. 871.

[7] Kestin, A. S., "Turbulent Diffusion of Heat and Mass in Catalytic Reactors for Hydrazine Decomposition," *Journal of Spacecraft and Rockets*, Vol. 7, No. 1, Jan. 1970, pp. 31–36.

[8] "Dynamic Analyses of Thrust Chambers," Interim Rept. 4600-147-1, Sept. 1968, Walter Kidde & Co., Belleville, New Jersey.

[9] Crocco, L., Grey, J., and Matthews, G. B., "Measurements of the Combustion Time Lag in a Liquid Bipropellant Rocket Motor," *Jet Propulsion*, Vol. 26, No. 1, Jan. 1956, pp. 20–25.

[10] Barrére, M., et al., "*Rocket Propulsion*," Van Nostrand, Princeton, 1960, pp. 630–632.

MARCH 1972 J. SPACECRAFT VOL. 9, NO. 3

Barrier Film Cooling Study

KURT BERMAN* AND S. J. ANDRYSIAK†
Bell Aerospace Company, Buffalo, N.Y.

Tests were conducted to evaluate the effectiveness of a liquid film barrier injected into a rocket thrust chamber with a vortex motion, insofar as heat transfer and performance were concerned. The propellant combination used was N_2O_4 and MMH. The engine, designed for a normal 450 lb thrust level at 125 psia chamber pressure, utilized a building block injector in which the core and barrier were fed separately, thus permitting independent control of the respective flow rates. The injector core pattern contained doublet and triplet elements. The chambers and nozzles were uncooled and instrumented with chromel-alumel thermocouples to obtain circumferential as well as axial heat rejection patterns. Both N_2O_4 and MMH were investigated as barrier coolants. Data were obtained showing the effect of barrier flow rate variations on performance and wall temperature at constant core flow rates and mixture ratios, as well as the effect of core flow mixture ratio variations on temperature and performance at constant barrier flow rates. This allowed the determination of the incremental effect of the two variables—barrier flow rate and core mixture ratio—on performance and heat transfer. Very good correlations were obtained. The effect of design modifications in the vortex barrier injection were also investigated. This paper will present the results of these experimental investigations and the correlation achieved.

Nomenclature

A_i, A_o = internal, external surface area of engine
c^* = over-all characteristic velocity
c_b^* = barrier effective characteristic velocity
c_c^* = core effective characteristic velocity
C_p = specific heat
k = thermal conductivity
h_g = heat-transfer coefficient
P_c = chamber pressure
q = heat flux rate
r = core mixture ratio
t = time
Tg, T_w, T_E = gas, wall, ambient environment temperature
V = volume of wall material
$\dot{W}_b$ = barrier flow rate
$\dot{W}_c$ = core flow rate
$\dot{W}_t$ = total propellant flow rate including barrier
x = axial length
ρ = $\dot{W}_b/\dot{W}_t, \rho = W_b$ and W_{FBT}.
σ = Stefan–Boltzmann constant
ϵ = emissivity
μ = density of wall material

Presented as Paper 71-676 at the AIAA/SAE 7th Propulsion Joint Specialist Conference, Salt Lake City, Utah, June 14–18, 1971; submitted June 23, 1971; revision received October 18, 1971. The authors wish to acknowledge the assistance of Palumbo and Blessing in the analysis of the heat-transfer data.

* Chief Engineer, Development and Technical. Fellow AIAA.
† Combustion Devices Engineer.

Introduction and Discussion

THE design of high-performance rocket engines requires that a thermal environment be provided near the engine walls which is compatible with the allowable steady-state temperature levels.[1] In general, this necessitates that the thermal potential of the combustion gas near the heat-transfer surfaces be significantly lower than that of the core products. The provision of a thermal barrier entails a loss in performance relative to what one might achieve if it were not needed. Therefore it is important to establish design parameters which permit meaningful tradeoffs between performance loss and acceptable driving temperatures. Two variables were evaluated in this investigation: 1) the type of barrier, i.e., fuel and oxidizer film; and 2) the utilization efficiency of the barrier as effected by its generation and quantity. A figure of merit must be measured in the capability of providing both uniform